Open Ceramics 17 (2024) 100541

Contents lists available at ScienceDirect

Open Ceramics

journal homepage: www.sciencedirect.com/journal/open-ceramics

Fast-firing of potassium sodium niobate (KNN)

Levent Karacasulu [a,b,*], Merve Karakaya [a], Umut Adem [a], Vincenzo M. Sglavo [b], Mattia Biesuz [b], Cekdar Vakifahmetoglu [a]

[a] Department of Materials Science and Engineering, İzmir Institute of Technology, 35430, İzmir, Türkiye
[b] Department of Industrial Engineering, University of Trento, Via Sommarive 9, 38123, Trento, Italy

ARTICLE INFO

Handling Editor: Dr P Colombo

Keywords:
Potassium sodium niobate
Fast-firing
Dielectric properties
Ferroelectric properties
Piezoelectric properties

ABSTRACT

Potassium sodium niobate (KNN) is one of the most promising Pb-free piezo-ceramics. In the present work, KNN was produced by fast-firing with different cooling strategies, i.e., fast and slow cooling. Dielectric, ferroelectric, and piezoelectric properties of fast-fired pellets were determined and compared with those of conventional-sintered products. Although the samples produced by fast-firing had higher density than those obtained by conventional sintering, fast-cooled samples following fast firing show relatively low electrical properties. When fast-firing was combined with slow cooling, the electrical properties, especially piezoelectric d_{33} values, were improved. The material subjected to fast-firing at 1120 °C using slow cooling gave the highest relative density (about 95 %) with fine grains microstructure and a d_{33} of 112 pC/N whereas that produced by conventional sintering resulted in d_{33} of 80 pC/N with a relative density of 88 % for the same dwell time (30 min).

1. Introduction

Firing has been used to densify ceramics for thousands of years. Traditionally, it consists of high-temperature treatment of a powder compact using heating rates ranging from a fraction to a few degrees Celsius per minute. For over half a century, unconventional sintering techniques have been proposed to enhance densification and/or suppress grain growth of ceramics [1].

Fast-firing (FF), introduced at the beginning of the '80s, is a very straightforward non-conventional sintering process. It enables densification by utilizing much higher heating rate (10^2–10^3 °C/min) with shorter dwell time [1,2]. In the fast-firing process, large heating rate has a vital role in enhancing densification and grain growth control, similar to other unconventional sintering techniques like spark-plasma, microwave and flash sintering [1]. For the same relative density, fast-fired samples are typically characterized by finer grain size, and reduced pore/grain boundary separation compared to those obtained by conventional sintering [1,3].

Fast-firing involves the direct introduction of the green sample into the hot zone of a furnace so that the ceramic quickly reaches the high-temperature regime. This allows the material to pass through the temperature region where grain coarsening is activated without densification in a few seconds/minutes. This phenomenon is associated with the different activation energies for the two processes, where densification (involving bulk/grain boundary diffusion) is typically characterized by higher activation energy than coarsening and, as such, requires a higher temperature for being activated [2,4,5]. Due to its "simplicity", FF resulted as a popular sintering technique with several industrial applications and has been used to sinter both traditional and advanced ceramics [6]. Fast firing was used for the densification of several systems, including traditional ceramics such as tiles and sanitaryware [7–9], technical ceramics such as alumina [10–13], barium titanate [14–17], ferrites [18], indium tin oxide [19], lanthanum gallate [20], lead magnesium niobate [21,22], lead zirconia titanate [23–26], zirconia [3,13,17,27–29], Sm_2O_3-doped CeO_2 [30], and even composites [31].

Potassium sodium niobate, $K_{0.5}Na_{0.5}NbO_3$ (KNN), has attracted tremendous attention in recent years as lead-free and environmental-friendly piezoelectric material. Besides showing a relatively high Curie temperature ($T_c \cong$ 418 °C), KNN is characterized by a large piezoelectric coefficient (d_{33} = 80 pC/N) when produced by conventional sintering [32,33]. In addition to that, reducing the particle size of the starting materials of pure KNN was observed to yield distinguishable results in d_{33} piezoelectric coefficients, increasing up to 107 pC/N [34]. The electrical properties of KNN are highly sensitive to the composition and this requires the maintenance of the desired stoichiometry during sintering [35–37]. Nevertheless, during conventional sintering with long dwell time, high density cannot be reached due to the volatilization of alkali elements and the formation of secondary phase [38,39]. In

* Corresponding author Department of Materials Science and Engineering, Izmir Institute of Technology, 35430, Izmir, Turkiye.
E-mail addresses: leventkaracasulu@iyte.edu.tr, leventkaracasulu@gmail.com (L. Karacasulu).

https://doi.org/10.1016/j.oceram.2024.100541
Received 27 August 2023; Received in revised form 21 December 2023; Accepted 11 January 2024
Available online 12 January 2024

addition, as a result of solid-state sintering (SSS) temperature (around 1120 °C) which approaches KNN melting point (1140 °C), lattice defects are generated and the stoichiometry might shift [40].

In the present study, fast-firing of KNN using powders produced by the solid-state synthesis was investigated for the first time. Dielectric, ferroelectric, and piezoelectric properties of the materials produced by FF were determined and compared with the conventional solid-state sintering process.

2. Experimental procedures

Nb_2O_5 (CAS#:12034-59-2, 99.9 %, Sigma–Aldrich, USA), Na_2CO_3 (CAS#:497-19-8, ≥ 99 %, Sigma Aldrich, USA) and K_2CO_3 (CAS#:584-08-7, ≥ 99.5 %, Sigma Aldrich, USA) precursors were weighed in accordance with the stoichiometric ratio and mixed in ethanol for 24 h using a planetary ball mill at 250 rpm (Retsch PM-100, Germany). After drying the slurry, calcination was carried out at 850 °C for 5 h in air, followed by ball-milling with zirconia spheres for 24 h.

The obtained powder was mixed with 10 wt% distilled water and uniaxially pressed under a pressure of 100 MPa within a steel die 8 mm in diameter. The green bodies with thickness of about 1.4 mm were dried overnight at 150 °C. The specimens were subjected to fast-firing using a tubular furnace (Nabertherm P330, Lilienthal, Germany) kept at various temperatures ranging from 1090 °C to 1130 °C. The samples were inserted quickly into the tube furnace at the selected temperature and kept there for 30 min. The fast-fired samples were extracted from the furnace in two ways. Some of them were quickly (~1 min) taken out from the furnace and cooled in air (cooling rate ~18 °C/s) - fast cooling (FC). Others were extracted in ~5 min (cooling rate ~4 °C/s) - slow cooling (SC). Some green samples were also conventionally sintered at the selected temperature for 30 min using 3 °C/min heating and cooling rate.

The bulk densitiy of the specimens was determined using water via the Archimedes' principle. Crystalline phases were identified using an X-ray diffractometer (XRD, Italstructures IPD3000 diffractometer, Italy) with Cu anode X-Ray source. XRD analysis were carried out in between 10° and 130° (2θ) range with 0.02° step size for a total of 1800s acquisition time. The morphology of the fracture surfaces was analyzed using scanning electron microscopy (SEM, FEI Quanta 250 FEG, USA). To measure the electrical properties, polished pellets produced by fast firing and conventional sintering were coated with silver paste on both surfaces and then cured at 200 °C for 20 min. The dielectric permittivity and loss variation with temperature was examined using an E4980AL LCR meter (Keysight Technologies, Santa Clara, CA, USA) at 100 kHz, from room temperature to 250 °C because the sample holder (aixACCT, TFA 423-7, Aachen, Germany) used for the dielectric measurement can endure up to 250 °C. The heating rate during measurement was 5 °C/min which was controlled by the temperature controller. The measurement was controlled with a Labview program. TF analyzer (aixACCT TF Analyzer 1000, Aachen, Germany), in conjunction with high voltage amplifier (TREK 610E, TREK, Medina, NY, USA) and laser-interferometer (SIOS Meβtechnik GmbH, Germany), was employed to generate P-E and S-E loops. The voltage applied during the P-E and S-E measurements was in the form of a triangular wave and was applied at 50 Hz. The frequency of 50 Hz was chosen because it was the maximum applicable frequency to suppress the leakage contribution to the hysteresis loops. To determine the piezoelectric coefficient (d_{33}), samples were poled under 40 kV/cm DC field at 25 °C for 10 min in a silicone oil bath and then analyzed using a Berlincourt type d_{33} meter (Sinocera Piezoelectronics, YE2730A, China). The poling procedure was carried out by using TF analyzer and high voltage amplifier which are same instruments mentioned above. The force applied via d_{33} meter has an amplitude of 0.25 N with 110 Hz frequency and the accuracy of the measurements in the range of 10–200 pC/N is ±5 %.

3. Results and discussion

The X-ray diffraction patterns of fast-fired and conventional sintered specimens are shown in Fig. 1 and compared to that of KNN powder synthesized by solid-state reaction. For all samples, no phase transformations or secondary phases are observed. All peaks are associated with the ICDD data of $K_{0.5}Na_{0.5}NbO_3$ (ICDD # 96-230-0500), presenting an orthorhombic structure. The KNN powder possesses single broader peaks with shoulders at larger angles, as it is generally observed for temperatures below 850 °C [41]. XRD peaks become narrower and sharper as the sintering temperature increases, pointing out the larger crystallinity of the system when compared to the as-synthesized powder.

The relative bulk density of FF samples is given in Fig. 2. While the sample sintered at 1090 °C show the lowest densification (87.3 %), a relative density of 93–94 % was obtained from specimens sintered at 1120–1130 °C, in proximity of the KNN melting point (1140 °C) [40]. Conventionally sintered samples treated at the same temperatures achieved lower densities than the fast-fired ones. The sample sintered at 1130 °C reaches a relative density of 91.7 %, the relative density clearly increasing with temperature.

Fig. 3 shows the fracture surface microstructure of fast-fired and conventionally sintered samples. The fracture surface of sample FFed at 1090 °C shows relatively small grains. The microstructure development with increasing temperature points out grain growth and, sometimes, abnormal grain growth, similarly to conventional sintering. Conversely, conventionally sintered samples show relatively low densification with cubic grains at 1090 and 1100 °C while grain growth begins at 1110 °C. At 1120 °C, dense microstructure appears with bimodal grain size consisting of fine cube-shaped grains and large grains exceeding 10 μm. While intergranular fracture predominated around the smaller grains, transgranular fracture is visible in the large grains, similarly to a previous study [42]. Indeed, this unique, abnormal grain growth phenomenon was observed in coarse KNN grains with specific core-shell structures. The core region consists of nano-sized grains, while the shell region has larger-sized similar self-assembled grains [43]. The extraordinary grain growth can be prevented by the FF because the activation energy for densification is higher than that for grain growth.

Fig. 4 demonstrates the temperature dependence of dielectric permittivity and dielectric loss (tan δ) at 100 kHz of KNN ceramics sintered at different temperatures by FF and CS methods. In general, the dielectric permittivity decreases when increasing the FF temperature. The O-T phase transition anomaly can be seen around 210 °C for all the samples (Fig. 4) [44]. On the other hand, the loss peaks of the FFed samples that appear at low temperatures (loss peaks are not visible for samples sintered at 1110 °C and 1120 °C) do not correspond to any phase transition. Still, they may show a relaxation behavior possibly resulting from the space-charge polarization effect or Schottky diode effect [45].

The dielectric permittivity and loss of samples produced by FF at 1090 and 1100 °C show similar behavior (Fig. 4(a)), while the sample fast-fired at 1110 °C has a lower dielectric permittivity and relatively low dielectric loss. A further decrease of the dielectric permittivity can be observed in the samples sintered at 1120 and 1130 °C. Higher dielectric loss values at low temperatures of the sample sintered at 1130 °C may indicate higher ion mobility or conductivity contribution and enhanced imperfections in the material [46,47]. To reduce the defects, controlled (slow) cooling was used for the FF samples. By using this approach, it was observed that the dielectric permittivities increased, but significant change was not observed in the loss behavior (dashed curves in Fig. 4(a)). Besides, the loss peaks at low temperatures were not observed in the samples produced by conventional sintering (Fig. 4(b)) characterized by lower loss values compared to fast-fired materials. The behaviours appear similar for all samples, the dielectric permittivity was increased with sintering temperature up to 1100 °C and then decreased. At 1130 °C, which is close to the melting temperature of KNN, the dielectric properties of CS samples start to deteriorate.

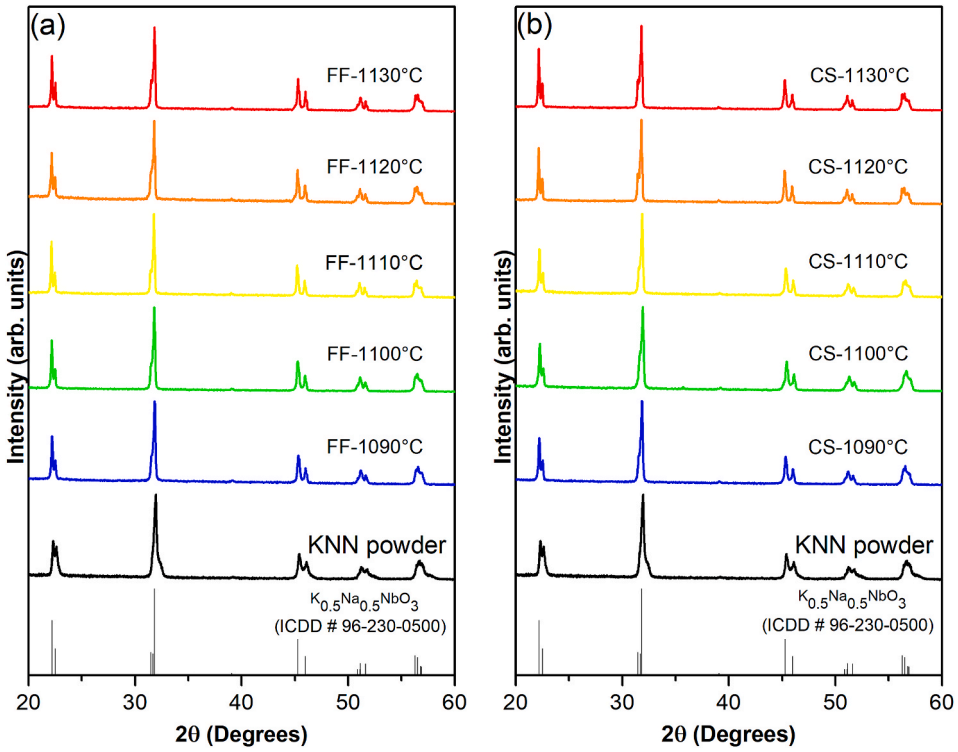

Fig. 1. X-ray diffraction patterns of KNN samples produced at different temperatures (1090–1130 °C) via **(a)** Fast-firing (FF) and **(b)** Conventional sintering (CS); the pattern recorded on the KNN powder synthesized via the solid-state reaction (KNN powder) is shown for comparison.

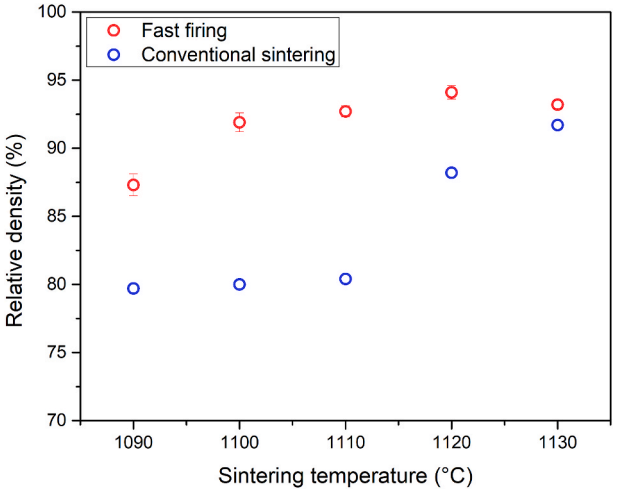

Fig. 2. Relative density of fast-fired and conventional sintered samples as a function of temperature.

Furthermore, samples conventionally sintered at 1110 and 1120 °C have the highest dielectric permittivity. It is important to note that the effects of sintering temperature and dwell time on electrical properties might be intricately influenced by grain size, compositional variation due to volatilization, ceramic density, and abnormal grain growth [43,48].

Fig. 5 shows the polarization-electric field hysteresis loops and strain-electric field curves. The FFed samples were measured at 50 Hz frequency to eliminate the conductivity contribution, as shown in Fig. 5 (a). However, specimens produced at 1110 and 1120 °C still exhibited high conductivity contribution and an artificial polarization value [44,45]. For such reason, their hysteresis loops are given only as insets on the graph. All loops, apart from those two, are pinched with low remanent polarization. Pinching of the loops was reported for KNN samples sintered via cold sintering, and it was ascribed to the pinning of domain walls by either point defects or fine grains [49]. It can also be seen from the dashed loop obtained at 1130 °C that the polarization values increased, and the lossy behavior decreased with slow cooling compared to fast cooling. In addition, the samples produced by fast firing-SC have higher strain values than those obtained by standard fast-firing. Polarization hysteresis loops of conventional sintered samples have a similar dielectric behavior trend (Fig. 4(b)). In addition, the trend in strain values of the CS samples is compatible with the dielectric and polarization properties, and the highest strain values belong to the samples sintered at 1110 and 1120 °C.

Fig. 6 reports the sintering temperature-dependent piezoelectric coefficients, d_{33} and d_{33}*. As can be seen, lower d_{33} values are obtained by standard fast-firing. The higher d_{33} values were obtained when fast-firing with slow cooling was carried out, thus reducing the defects and, hereof, the conductivity contribution. If the cooling rate is high and the defect removal rate is slow, high defect concentrations can be present at room temperature, thus influencing the ferroelectric and piezoelectric properties [50]. Reduced defect concentration can facilitate domain wall motion and increase extrinsic contribution to piezoelectricity. In addition, smaller grain size of the FFed samples might also be increasing d_{33} coefficient, as domain wall concentration is expected to increase with decreasing grain size. It is worth noting that d_{33} coefficients of typical highly dense KNN ceramics produced by conventional sintering usually range between 80 and 110 pC/N (e.g., 80 pC/N at 1120 °C found in this study) [51], reaching 160 pC/N with a relative density of around 99 % by hot pressing [33]. The d_{33} value of the sample subjected to FF at 1120 °C is 49 pC/N, while material fast-fired at 1120 °C with slow cooling yields 112 pC/N, exceeding typical d_{33} values of conventional ones. The d_{33} value of samples conventionally sintered at 1130 °C, which approaches the melting temperature of KNN, is found to be relatively low, similar to the obtained dielectric properties. It should be noted that the measured samples produced by both techniques usually exhibited transgranular fracture, indicating the grain boundaries with a weaker path for crack propagation. The coefficient of d_{33} might be enhanced

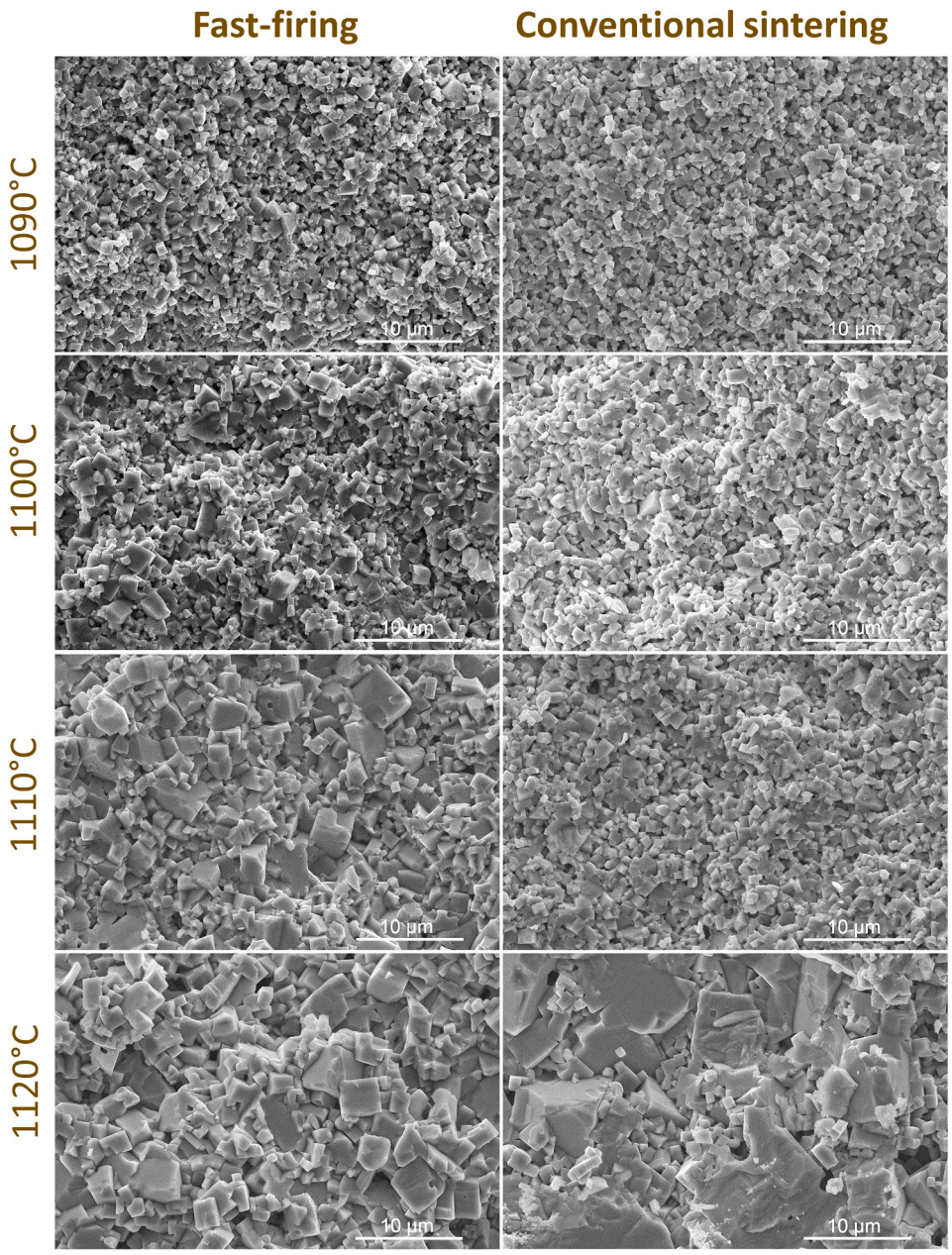

Fig. 3. Fracture surface morphologies of conventional sintered and fast-fired samples at 1090 °C, 1100 °C, 1110 °C and 1120 °C.

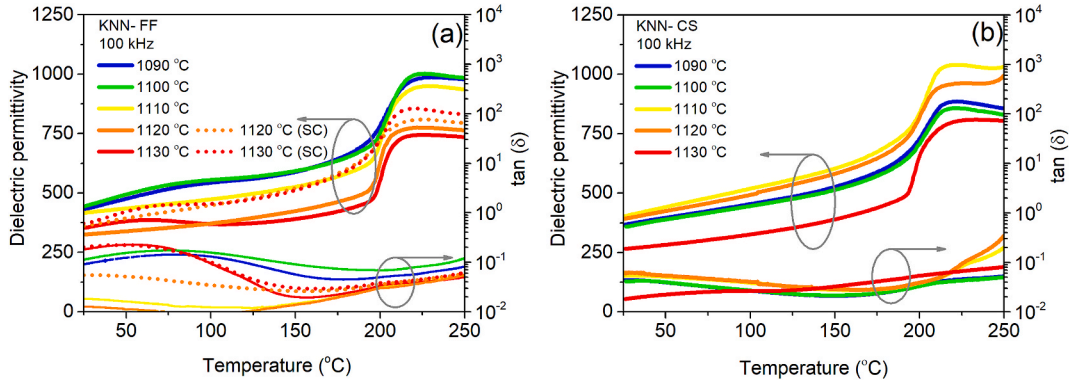

Fig. 4. Temperature dependence of the dielectric permittivity and dielectric loss (tan δ) of KNN ceramics produced by **(a)** fast-firing and fast-firing with slow cooling (SC) and **(b)** conventional sintering.

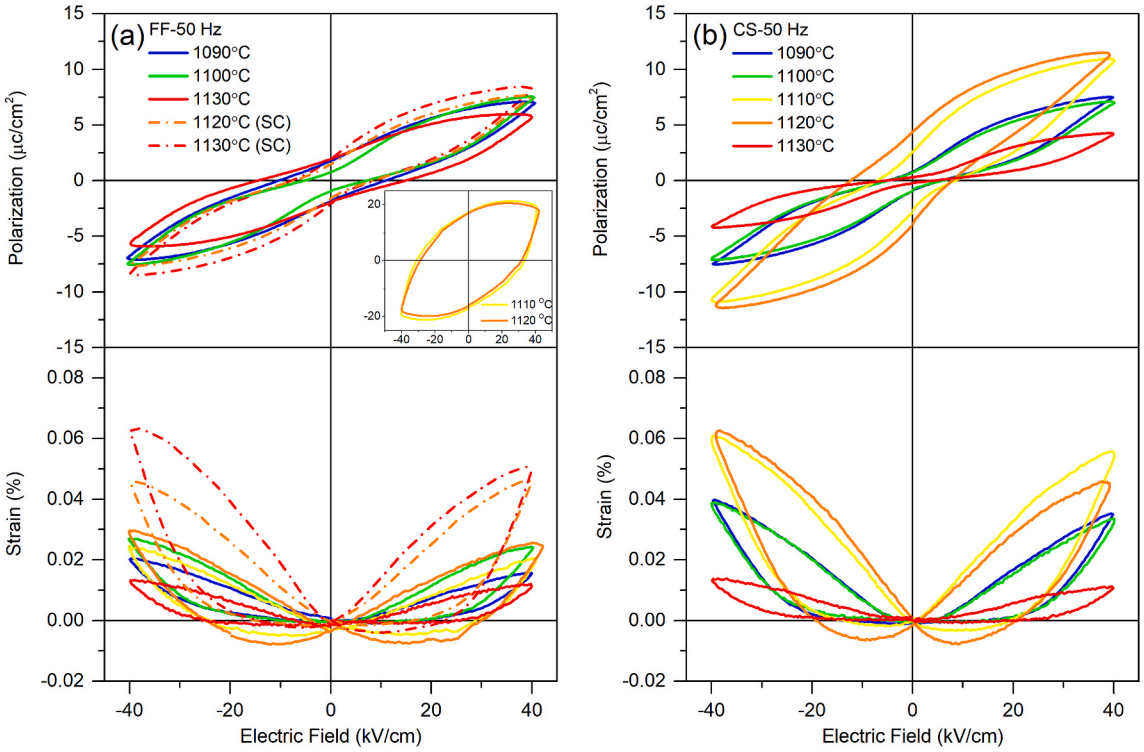

Fig. 5. Polarization-electric field hysteresis loops and strain-electric field curves of KNN sintered by **(a)** fast-firing and fast-firing with slow cooling (SC) and **(b)** conventional sintering at different temperatures.

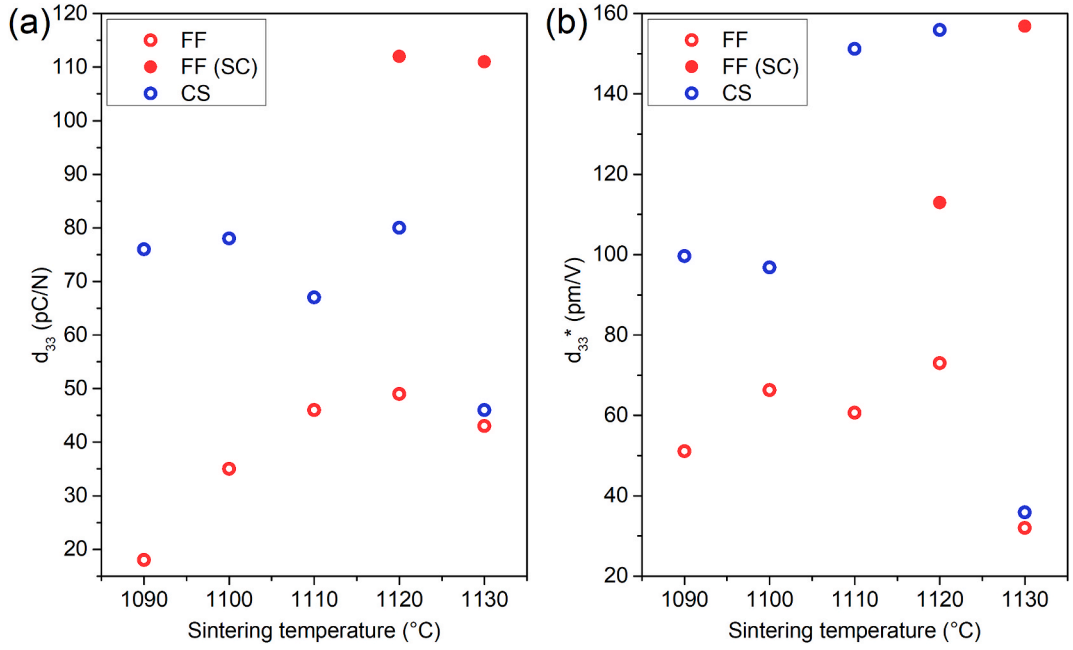

Fig. 6. Sintering temperature-dependent piezoelectric coefficients of samples produced by fast-firing (FF), fast-firing with slow cooling (SC), and conventional sintering (CS): **(a)** d_{33} and **(b)** d_{33}*.

with the introduction of crack formation during poling [52]. Therefore, d_{33}* values were also calculated by utilizing strain measurements. d_{33}* values, as shown in Fig. 6(b), which are derived from the expression d_{33}* = (max strain)/(applied electric field), are usually consistent with the d_{33} values [53]. The d_{33}* values of conventional sintered KNN were found to be 86–112 pm/V when sintered under an air atmosphere and 119 pm/V when sintered under a low O_2 atmosphere in the previous work [54]. These values are comparable with this work, especially for conventional sintered and fast-fired with slow cooling samples.

4. Conclusions

Potassium sodium niobate (KNN) ceramics were densified by fast-firing at 1090–1130 °C for 30 min. While higher relative densities

were obtained by FF compared to conventional sintering, the fast-fired pellets demonstrated relatively low electrical properties. When FF with slow cooling was carried out, dielectric, polarization, and piezoelectric properties were enhanced. While the material produced by conventional sintering had a d_{33} of 80 pC/N with a relative density of 88 % (1120 °C), FF at 1120°C led to higher relative density (about 95 %) with a smaller grain size. If FF was followed by controlled cooling, d_{33} as high as 112 pC/N can be obtained.

Declaration of competing interest

The authors declare that they have no known competing financial interests or personal relationships that could have appeared to influence the work reported in this paper.

Acknowledgments

The authors are grateful to the JECS Trust for funding [the visit of Levent Karacasulu to the University of Trento] (Contract No. 2021283). We acknowledge the Izmir Institute of Technology, Center for Materials Research for SEM investigations. This research has been funded by the Italian Ministry for University and Research (MUR) through the "Departments of Excellence 2023–27" program (L.232/2016) awarded to the Department of Industrial Engineering of the University of Trento.

References

[1] R.K. Bordia, S.-J.L. Kang, E.A. Olevsky, Current understanding and future research directions at the onset of the next century of sintering science and technology, J. Am. Ceram. Soc. 100 (2017) 2314–2352, https://doi.org/10.1111/jace.14919.
[2] M.P. Harmer, R.J. Brook, Fast firing-microstructural benefits, Trans. J. Br. Ceram. Soc. 80 (1981) 147–148.
[3] D.-H. Kim, C.H. Kim, Effect of heating rate on pore shrinkage in yttria-doped zirconia, J. Am. Ceram. Soc. 76 (1993) 1877–1878, https://doi.org/10.1111/j.1151-2916.1993.tb06665.x.
[4] A. Leriche, F. Cambier, S. Hampshire, Sintering of ceramics, in: Reference Module in Materials Science and Materials Engineering, Elsevier, 2017, https://doi.org/10.1016/B978-0-12-803581-8.10288-7.
[5] S.-J.L. Kang, What we should consider for full densification when sintering, Materials 13 (2020) 3578.
[6] D. Hotza, D.E. García, R.H.R. Castro, Obtaining highly dense YSZ nanoceramics by pressureless, unassisted sintering, Int. Mater. Rev. 60 (2015) 353–375, https://doi.org/10.1179/1743280415Y.0000000005.
[7] H. Moertel, Porcelain for fast firing, Ceramurg. Int. 3 (1977) 65–69, https://doi.org/10.1016/0390-5519(77)90032-1.
[8] P.I. Berenshtein, Fast single firing of ceramic tiles, Glass Ceram. 33 (1976) 36–38, https://doi.org/10.1007/BF00702046.
[9] V. Viswabaskaran, F.D. Gnanam, Development of fast firing vitreous sanitaryware, Trans. Indian Ceram. Soc. 59 (2000) 105–108, https://doi.org/10.1080/0371750X.2000.10799942.
[10] D.E. García, J. Seidel, R. Janssen, N. Claussen, Fast firing of alumina, J. Eur. Ceram. Soc. 15 (1995) 935–938, https://doi.org/10.1016/0955-2219(95)00071-2.
[11] D.E. García, D. Hotza, R. Janssen, Building a sintering front through fast firing, Int. J. Appl. Ceram. Technol. 8 (2011) 1486–1493, https://doi.org/10.1111/j.1744-7402.2011.02609.x.
[12] T.S. Possamai, R. Oba, V.P. Nicolau, D. Hotza, D.E. García, Numerical simulation of the fast firing of alumina in a box furnace, J. Am. Ceram. Soc. 95 (2012) 3750–3757, https://doi.org/10.1111/j.1551-2916.2012.05432.x.
[13] V. Prajzler, D. Salamon, K. Maca, Pressure-less rapid rate sintering of pre-sintered alumina and zirconia ceramics, Ceram. Int. 44 (2018) 10840–10846, https://doi.org/10.1016/j.ceramint.2018.03.132.
[14] H. Mostaghaci, R.J. Brook, Microstructure development and dielectric properties of fast-fired $BaTiO_3$ ceramics, J. Mater. Sci. 21 (1986) 3575–3580, https://doi.org/10.1007/BF00553803.
[15] W. Zhu, C.C. Wang, S.A. Akbar, R. Asiaie, Fast-sintering of hydrothermally synthesized $BaTiO_3$ powders and their dielectric properties, J. Mater. Sci. 32 (1997) 4303–4307, https://doi.org/10.1023/A:1018663621241.
[16] A. Bologna Alles, R. Vanalstine, W. Schulze, Dielectric properties and aging of fast-fired barium titanate, Lat. Am. Appl. Res. 35 (2005) 29–35.
[17] V. Bijalwan, V. Prajzler, J. Erhart, J.J. Velazquez, D. Galusek, K. Maca, Rapid pressureless sintering of barium titanate–based piezoceramics and their electromechanical harvesting performance, J. Am. Ceram. Soc. 105 (2022) 6886–6897, https://doi.org/10.1111/jace.18602.
[18] A. Dias, Microstructural evolution of fast-fired nickel–zinc ferrites from hydrothermal nanopowders, Mater. Res. Bull. 35 (2000) 1439–1446, https://doi.org/10.1016/S0025-5408(00)00337-8.
[19] B.-C. Kim, J.-H. Lee, J.-J. Kim, H.Y. Lee, J.-S. Lee, Densification of nanocrystalline ITO powders in fast firing: effect of specimen mass and sintering atmosphere, Mater. Res. Bull. 40 (2005) 395–404, https://doi.org/10.1016/j.materresbull.2004.10.006.
[20] S.L. Reis, E.N.S. Muccillo, Microstructure and electrical conductivity of fast fired Sr- and Mg-doped lanthanum gallate, Ceram. Int. 42 (2016) 7270–7277, https://doi.org/10.1016/j.ceramint.2016.01.121.
[21] S.M. Landin, W.A. Schulze, Rapid thermal processing of $Pb(Mg_{0.7}Zn_{0.3})_{1/3}Nb_{2/3}O_3$ multilayer ceramic capacitors, J. Am. Ceram. Soc. 73 (1990) 909–912, https://doi.org/10.1111/j.1151-2916.1990.tb05134.x.
[22] S.M. Landin, W.A. Schulze, Rapid sintering of stoichiometric zinc-modified lead magnesium niobate, J. Am. Ceram. Soc. 73 (1990) 913–918, https://doi.org/10.1111/j.1151-2916.1990.tb05135.x.
[23] C.E. Baumgartner, Fast firing and conventional sintering of lead zirconate titanate ceramic, J. Am. Ceram. Soc. 71 (1988) C-350–C-353, https://doi.org/10.1111/j.1151-2916.1988.tb05939.x.
[24] C.-C. Hsueh, M.L. Mecartney, W.B. Harrison, M. Renee, B. Hanson, B.G. Koepke, Microstructure and electrical properties of fast-fired lead zirconate-titanate ceramics, J. Mater. Sci. Lett. 8 (1989) 1209–1216, https://doi.org/10.1007/BF01730072.
[25] C.R. Bowen, J. Open, J. Fitzmaurice, S. Mahon, Fast firing of electroceramics, Ferroelectrics 228 (1999) 159–166, https://doi.org/10.1080/00150199908226133.
[26] A. Seal, R. Mazumder, A. Sen, H.S. Maiti, Fast firing of lead zirconate titanate ceramics at low temperature, Mater. Chem. Phys. 97 (2006) 14–18, https://doi.org/10.1016/j.matchemphys.2005.05.038.
[27] S.Y. Gómez, A.L. da Silva, D. Gouvêa, R.H.R. Castro, D. Hotza, Nanocrystalline yttria-doped zirconia sintered by fast firing, Mater. Lett. 166 (2016) 196–200, https://doi.org/10.1016/j.matlet.2015.12.042.
[28] V. Prajzler, S. Průša, K. Maca, Rapid pressure-less sintering of fine grained zirconia ceramics: explanation and elimination of a core-shell structure, J. Eur. Ceram. Soc. 39 (2019) 5309–5319, https://doi.org/10.1016/j.jeurceramsoc.2019.07.053.
[29] W. Ji, B. Parker, S. Falco, J.Y. Zhang, Z.Y. Fu, R.I. Todd, Ultra-fast firing: effect of heating rate on sintering of 3YSZ, with and without an electric field, J. Eur. Ceram. Soc. 37 (2017) 2547–2551, https://doi.org/10.1016/j.jeurceramsoc.2017.01.033.
[30] M. Biesuz, L. Spiridigliozzi, M. Frasnelli, G. Dell'Agli, V.M. Sglavo, Rapid densification of Samarium-doped Ceria ceramic with nanometric grain size at 900–1100°C, Mater. Lett. 190 (2017) 17–19, https://doi.org/10.1016/j.matlet.2016.12.132.
[31] D.E. García, J. Wendorff, R. Janssen, N. Claussen, Fast firing of reaction-bonded aluminium oxide RBAO composites, J. Mater. Sci. 30 (1995) 5121–5124, https://doi.org/10.1007/BF00356058.
[32] L. Egerton, D.M. Dillon, Piezoelectric and dielectric properties of ceramics in the system potassium—sodium niobate, J. Am. Ceram. Soc. 42 (1959) 438–442.
[33] R.E. Jaeger, L. Egerton, Hot pressing of potassium-sodium niobates, J. Am. Ceram. Soc. 45 (1962) 209–213.
[34] R. Zuo, J. Rödel, R. Chen, L. Li, Sintering and electrical properties of lead-free $Na_{0.5}K_{0.5}NbO_3$ piezoelectric ceramics, J. Am. Ceram. Soc. 89 (2006) 2010–2015, https://doi.org/10.1111/j.1551-2916.2006.00991.x.
[35] C. Piskin, L. Karacasulu, M. Bortolotti, C. Vakifahmetoglu, Synthesis of potassium–sodium niobate (KNN) from NbO_2, Open Ceramics 7 (2021) 100159, https://doi.org/10.1016/j.oceram.2021.100159.
[36] C. Piskin, L. Karacasulu, G. Ischia, M. Bortolotti, C. Vakifahmetoglu, Hydrothermal synthesis of potassium–sodium niobate powders, J. Am. Ceram. Soc. 105 (2022) 3809–3819, https://doi.org/10.1111/jace.18349.
[37] L. Karacasulu, C. Vakifahmetoglu, Cold sintering assisted two-step sintering of potassium sodium niobate (KNN) ceramics, Mater. Sci. Eng. B 297 (2023) 116709, https://doi.org/10.1016/j.mseb.2023.116709.
[38] B. Malič, J. Koruza, J. Hreščak, J. Bernard, K. Wang, J.G. Fisher, A. Benčan, Sintering of lead-free piezoelectric sodium potassium niobate ceramics, Materials 8 (2015) 8117–8146.
[39] M. Bah, R. Podor, R. Retoux, F. Delorme, K. Nadaud, F. Giovannelli, I. Monot-Laffez, A. Ayral, Real-time capturing of microscale events controlling the sintering of lead-free piezoelectric potassium-sodium niobate, Small 18 (2022) 2106825, https://doi.org/10.1002/smll.202106825.
[40] R. López, F. González, M.P. Cruz, M.E. Villafuerte-Castrejon, Piezoelectric and ferroelectric properties of $K_{0.5}Na_{0.5}NbO_3$ ceramics synthesized by spray drying method, Mater. Res. Bull. 46 (2011) 70–74.
[41] P. Bomlai, P. Wichianrat, S. Muensit, S.J. Milne, Effect of calcination conditions and excess alkali carbonate on the phase formation and particle morphology of $Na_{0.5}K_{0.5}NbO_3$ powders, J. Am. Ceram. Soc. 90 (2007) 1650–1655, https://doi.org/10.1111/j.1551-2916.2007.01629.x.
[42] D. Jenko, A. Benčan, B. Malič, J. Holc, M. Kosec, Electron microscopy studies of potassium sodium niobate ceramics, Microsc. Microanal. 11 (2005) 572–580.
[43] Y. Zhen, J.-F. Li, Abnormal grain growth and new core–shell structure in (K,Na)NbO_3-based lead-free piezoelectric ceramics, J. Am. Ceram. Soc. 90 (2007) 3496–3502, https://doi.org/10.1111/j.1551-2916.2007.01977.x.
[44] Y. Su, X. Chen, Z. Yu, H. Lian, D. Zheng, J. Peng, Comparative study on microstructure and electrical properties of $(K_{0.5}Na_{0.5})NbO_3$ lead-free ceramics prepared via two different sintering methods, J. Mater. Sci. 52 (2017) 2934–2943, https://doi.org/10.1007/s10853-016-0587-z.
[45] K. Datta, K. Roleder, P.A. Thomas, Enhanced tetragonality in lead-free piezoelectric $(1-x)BaTiO_3$–$xNa_{1/2}Bi_{1/2}TiO_3$ solid solutions where x=0.05–0.40, J. Appl. Phys. 106 (2009) 123512, https://doi.org/10.1063/1.3268443.
[46] M.E. Lines, A.M. Glass, Principles and Applications of Ferroelectrics and Related Materials, Oxford university press, 2001.

[47] P. Kumar, M. Pattanaik, Sonia, Synthesis and characterizations of KNN ferroelectric ceramics near 50/50 MPB, Ceram. Int. 39 (2013) 65–69, https://doi.org/10.1016/j.ceramint.2012.05.093.
[48] R. Serrazina, A. Tkach, L. Pereira, A.M.O.R. Senos, P.M. Vilarinho, Flash sintered potassium sodium niobate: high-performance piezoelectric ceramics at low thermal budget processing, Materials 15 (2022) 6603.
[49] K. Tsuji, Z. Fan, S.H. Bang, S. Dursun, S. Trolier-McKinstry, C.A. Randall, Cold sintering of the ceramic potassium sodium niobate, $(K_{0.5}Na_{0.5})NbO_3$, and influences on piezoelectric properties, J. Eur. Ceram. Soc. 42 (2022) 105–111, https://doi.org/10.1016/j.jeurceramsoc.2021.10.002.
[50] A.J. Moulson, J.M. Herbert, Electroceramics: Materials, Properties, Applications, John Wiley & Sons, 2003.
[51] H. Birol, D. Damjanovic, N. Setter, Preparation and characterization of $(K_{0.5}Na_{0.5})NbO_3$ ceramics, J. Eur. Ceram. Soc. 26 (2006) 861–866.
[52] J. Mendiola, C. Alemany, L. Pardo, A. Gonzalez, Poling reversal effects on piezoelectricity of calcium modified lead titanate ceramic, Ferroelectrics 94 (1989) 209–214, https://doi.org/10.1080/00150198908014255.
[53] Y. Zhao, Z. Xu, R. Chu, J. Hao, J. Du, G. Li, Improved piezoelectricity and high strain response of $(1-x)(0.948K_{0.5}Na_{0.5}NbO_3 - 0.052LiSbO_3) - xBi_2O_3$ ceramics, J. Mater. Sci. Mater. Electron. 28 (2017) 1211–1216, https://doi.org/10.1007/s10854-016-5647-2.
[54] Z. Yu, X. Chen, H. Lian, Q. Zhang, W. Wu, Microstructure and electrical properties of $K_{0.5}Na_{0.5}NbO_3$ lead-free piezoelectric ceramics sintered in low pO_2 atmosphere, J. Mater. Sci. Mater. Electron. 29 (2018) 19043–19051, https://doi.org/10.1007/s10854-018-0030-0.